Article

Not peer-reviewed version

# Ameliorative Inhibition of SIRT6 by Imidazole Derivative Triggers Oxidative Stress-Mediated Apoptosis Associated with Nrf2/Keap1 Signaling in NSCLC Cell Lines

Uma Maheswara Rao Dindi , Sammer Al-Ghamdi , Naif Alrudian , Bin Dayelb Salman , Abdulwahab A. Abuderman , Shahidc Mohammad , Thiyagarajan Ramesh * , Ravikumar Vilwanathan *

Posted Date: 7 August 2023

doi: 10.20944/preprints202308.0482.v1

Keywords: Epigenetics; SIRT6; HDAC; HDACi; KEAP1; NRF2

*Article*

# Ameliorative Inhibition of SIRT6 by Imidazole Derivative Triggers Oxidative Stress-Mediated Apoptosis Associated with Nrf2/Keap1 Signaling in NSCLC Cell Lines

**Dindi Uma Maheswara Rao [1], Sameer Al-Ghamdia [2], Naif Abdurhman Alrudiana [2], Salman Bin Dayelb [3], Abdulwahab Ali Abudermanc [4], Mohammad Shahidc [4], Thiyagarajan Ramesh [4,*] and Ravikumar Vilwanathan [1,*]**

[1] Department of Biochemistry, Cancer Biology Laboratory, School of Life Sciences, Bharathidasan University, Tiruchirappalli- 620 024, Tamil Nadu, India.
[2] Department of Family and Community Medicine, College of Medicine, Prince Sattam Bin Abdulaziz University, Al-Kharj-11942, Saudi Arabia.
[3] Dermatology Unit, Internal Medicine Department, College of Medicine, Prince Sattam Bin Abdulaziz University, Al-Kharj-11942, Kingdom of Saudi Arabia.
[4] Department of Basic Medical Sciences, College of Medicine, Prince Sattam Bin Abdulaziz University, Al-Kharj-11942, Kingdom of Saudi Arabia
* Correspondence: Dr. Ravikumar Vilwanathan Email: ravikumarbdu@gmail.comPhone: +91-0431-2407071 (570) Fax: +91-0431-2407045 and Dr. Thiyagarajan Ramesh Email: r.thiyagarajan@psau.edu.sa

**Highlights**

- Ethyl [5-(4-Chlorophenyl)-2-methyl-1H-imidazol-4-yl}-acetate effect on Lung cancer cell lines A549 and NIC-H460.
- SIRT6 inhibition by Ethyl [5-(4-Chlorophenyl)-2-methyl-1H-imidazol-4-yl}-acetate.
- Nrf2/Keap1 signaling modulation through SIRT6 inhibition.
- Ethyl [5-(4-Chlorophenyl)-2-methyl-1H-imidazol-4-yl}-acetate induced oxidative stress and apoptosis.

**Abstract:** The nuclear factor-erythroid 2 p45-related factor 2 (Nrf2, also called Nfe2l2)/Kelchlike ECH-associated protein 1 (Keap1) signaling is the major regulator of redox homeostasis. The imbalance of redox homeostasis causes oxidative stress. Keap1 is the one that regulates Nrf2 by binding to Nrf2. Nrf2/Keap1 signaling is reported to be involved in cancer cell growth and survival. The high level of Nrf2 in cancers is associated with poor prognosis, resistance to therapeutics and rapid proliferation framing Nrf2 as an interesting target in cancer biology. Sirtuins (SIRT1-7) are class III histone deacetylases with NAD+-dependent deacetylase activity. High levels of SIRT6 are contributing to cancer progression in many types of human tumors, and its overexpression has been reported to involve positive modulation of the Nrf2/Keap1 pathway, suggesting SIRT6 is a key regulator of this Nrf2/Keap1 Signaling. The natural or synthetic compound that inhibits key regulators of Nrf2 signaling becomes an attractive target. In the present study, we investigated the pharmacological effect of Ethyl (5-(4-Chlorophenyl)-2-methyl-1H-imidazol-4-yl) - acetate an imidazole derivative on Nrf2/Keap1 in A549 and NIC-H460 cell lines. Imidazole derivative inhibited the SIRT6 expression at gene and protein levels. The gene and protein expression of Nrf2 and Keap1 were modulated during SIRT6 inhibition. The level of anti-oxidant enzymes such as GSH, GPx, Catalase, and % ROS scavenging activity were depleted upon SIRT6 inhibition. Further, morphological studies support ROS generation, mitochondrial damage, nuclear damage, and apoptosis. The molecular examination of apoptosis by gene and protein expression of apoptotic factors confirms apoptotic cell death. Our results suggest that the Imidazole derivative affects Nrf2/Keap1 signaling by targeting SIRT6 might be a new promising approach to cancer treatment opportunity for disrupting Nrf2/Keap1 signaling in lung cancer.

 doi:10.20944/preprints202308.0482.v1



**Keywords:** Epigenetics; SIRT6; HDAC; HDACi; KEAP1; NRF2

## 1. Introduction

Lung cancer is the leading cause of cancer deaths worldwide. Lung cancer is classified into two main types, Non- small-cell lung carcinoma (NSCLC, 85%) and small-cell lung carcinoma (SCLC, 25%). NSCLC is the most common with three main types including adenocarcinoma 40%, squamous 25-30%, and large cell 5-10% [1]. Various phenotypic manifestations are associated with the onset of cancer while oxidative stress plays a crucial role in the progression of tumorigenesis by impairment of important pathways in DNA repair, cell survival, and proliferation favoring genetic and/or epigenetic dysregulation of oncogenes and tumor suppressor genes [2]. In normal cells-controlled production of reactive oxidants was delivered to fulfill the much-needed purpose of regulating signaling pathways which are counterbalanced by an antioxidant defense system ensuring the adequate response whenever needed by the body [3]. Oxidative stress is generated due to an imbalance between highly reactive molecules called Reactive oxygen species (ROS), such as superoxide (O2−), hydroxyl radical (OH−), and hydrogen peroxide (H2O2) and antioxidants namely, superoxide dismutase, catalases, thioredoxins, peroxiredoxins, reductases and peroxidases [4]. ROS exposure prompts the production of antioxidant enzymes even ROS can also be neutralized by non-enzymatic compounds such as glutathione, coenzyme Q and lipoic acid prevents oxidative stress by quenching ROS [5]. Oxidative stress thus plays a pivotal role in determining cell fate to promote normal cell death in response to excessive ROS production, however, in carcinogenesis high amount of ROS promotes defective signaling factors through the deregulation of biomolecules. Therefore, factors able to initiate cellular rescue pathways in transformed cells as a response to oxidative stress stimuli are actively considered potential prognostic factors and possible therapeutic targets.

The nuclear factor erythroid-2-related factor 2/ Kelch-like ECH-associated protein 1 (Nrf2/Keap1) is the major regulator of cellular homeostasis in response to xenobiotic and oxidative stress [6]. Nrf2 initiates cellular rescue pathways against oxidative injury, inflammation/immunity, apoptosis, and carcinogenesis. Under normal conditions, Nrf2 is constitutively expressed and degraded in the cytoplasm. Keap1 is the one that mediates the polyubiquitination and degradation of Nrf2 through the Cul3 E3 ligase complex [7]. On oxidative stress, Keap1 cysteine residues undergo a conformational change, which disassociates Keap1 binding to Nrf2 and prevents degradation leading to the accumulation of Nrf2 in the cytosol [8]. Nrf2 moves to the nucleus and binds to Antioxidant Response Element (ARE) in the promoter region of antioxidant regulatory genes and protects cells from oxidative damage by transcriptionally activating antioxidant genes [9]. Nrf2 protects both normal cells and cancer cells from cellular stresses [10]. In normal cells, Nrf2 activation prevents DNA damage and mutations which can initiate carcinogenesis. Whereas Nrf2 in transformed cells supports tumor progression by protecting against oxidative damage [11]. The constitutive expression of Nrf2 creates a redox environment that facilitates tumor growth and promotes resistance to chemotherapy. High levels of Nrf2 are associated with poor prognosis [12], [13]. Dysregulation of Nrf2/Keap1, is reported in several tumors, including NSCLC. The functional loss of Keap1 leads to constitutive expression of Nrf2 in about 19% of tumors and up to 50% of NSCLC cell lines [14]. Nrf2 upregulation and Keap1 down-regulation are common abnormalities in NSCLC and are associated with poor prognosis [15].

Regulation of NRF2 signaling has been established to occur at the level of transcription, post-transcription, and protein stability. Although genetic alterations initially were reported in Nrf2/Keap1, more recently, epigenetic modifications have added a new dimension and an element of fine-tuning to the Nrf2 signaling axis [16]. This was well supported by a study indicating that epigenetic modulation of Histone deacetylases (HDACs) inhibition leads to the regulation of Nrf2 expression at the transcriptional level [17]. HDACs are classified under a group of histone regulatory enzymes that are accountable for the removal of the acetyl group from ε-N –acetyl lysine amino acid residues from histone as well as non-histone proteins. There are 18 HDACs that have been discovered

 doi:10.20944/preprints202308.0482.v1



in humans. HDACs have been classified into two families (classical and sirtuins) and categorized into four classes (Class 1, Class 2, Class 3, and Class 4). Sirtuins belong to Class 3 Histone deacetylases with highly conserved NAD+ domain, having high sequence similarity with the yeast Saccharomyces cerevisiae Protein Sir2 (silent information regulator 2) and having no sequence similarity with classical HDACs. Sirtuins like classical HDACs catalyze post-translational modification of histone and non-histone proteins. There are seven types of sirtuins reported in humans, differing in localization, enzymatic activities, and targets. SIRT1 and SIRT6 are found predominantly in the nucleus, SIRT2 is found in the cytoplasm, and SIRT3, SIRT4, and SIRT5 are found in mitochondria [18].

Among the class of Sirtuins, SIRT6 has a dual role of tumorigenesis and tumor suppression, this depends on the specific context and the type of cancer [19]. We previously reported that the knocked down of SIRT6 induced cell cycle arrest and apoptosis in NSCLC cells [20]. Oxidative stress is reported to be involved in tumor initiation and progression [21]. SIRT6 has been reported to play a prominent role in promoting cancer cell survival under oxidative stress confirming its role in redox-related cellular homeostasis. SIRT6 acts as a key regulator of oxidative stress and counteracts oxidative stress by regulating the expression and activity of antioxidant enzymes, such as superoxide dismutase (SOD), catalase, and ROS detoxification. This provides a survival advantage to cancer cells that are exposed to high levels of ROS [22]. The Nrf2/Keap1 pathway is a pivotal player in the signaling cascade responsible for the resistance of oxidative damage. Recent evidence suggests that Nrf2 has an aberrant activation of Nrf2 associated with poor prognosis with a contrasting role in cancers. Aberrant activation of Nrf2 is associated with poor prognosis can inhibit apoptosis and promotes tumor proliferation.

SIRT6 is very well involved in the regulation of nuclear factor erythroid 2-related factor 2 (Nrf2). SIRT6 deficiency decreases the Nrf2 protein levels and the mRNA levels of its target genes whereas SIRT6 over-expression increased the Nrf2 protein content [23]. Considering the key regulating role of SIRT6 on Nrf2 oxidative stress in transformed cells, SIRT6 might be a potential target for countering Nrf2-mediated cellular rescue pathways in tumor cells, and implementation of effective SIRT6 inhibitors will effectively suppress Nrf2-mediated cellular rescue pathways. Generally, heterocyclic compounds with nitrogen atoms have a broad range of pharmaceutical activities [24]. According to reports, 59% of small-molecule agents approved by the FDA have nitrogen-containing heterocyclic rings [25]. Imidazole is an aromatic compound with five-membered heterocyclic rings and two nitrogen atoms that preserve an important class of therapeutic agents in current medicinal science [26]. Imidazole's pharmacological properties, in particular anticancer activity, attracted the development of imidazole derivatives-based anticancer drugs with increasing efficiency and lowering the side effects [27]. The modifications by the addition of substituents to the imidazole ring can alter its pharmacokinetics properties, allowing for improved interactions of the imidazole derivative. Recently, the pyrrole-pyridinimidazole derivative is reported as a potent SIRT6 inhibitor with a promising non-competitive inhibition profile in pancreatic cancer cells [28]. We too performed a virtual screening study on binding pattern analysis of a series of imidazole derivatives for its inhibitory effect on SIRT6 [29].

Since SIRT6 is very well involved in the regulation of Nrf2 and implementation of effective SIRT6 inhibitors will efficiently suppress Nrf2 mediated cellular rescue pathways in tumor cells. Herein, we hypothesized to evaluate the regulatory effect of Ethyl (5-(4-Chlorophenyl)-2-methyl-1H-imidazol-4-yl) – acetate on Nrf2/Keap1 signaling pathway in NSCLC cell lines.

## 2. Materials and Methods

### *2.1. Cell culture*

The human non-small-cell lung cancer cell lines, A549 (adenocarcinoma) and NCI-H460 (squamous cell carcinoma) were purchased from National Centre for Cell Science (NCCS) Pune, India. The cell culture reagents such as Dulbecco's Modified Eagle's Medium (DMEM), Fetal bovine serum (FBS), 10X Phosphate Buffered Saline (pH 7.2), 10X Trypsin-EDTA, 100X penicillin-

streptomycin (pen/strep, pH 7.2) antibiotic solution from Hi-Media Laboratories, Mumbai, India. Cell culture plates were purchased from Wuxi NEST Biotechnology Co. Ltd, Jiangsu, China. The other plastic wares were purchased from Tarsons PVT LTD.

The cell lines were cultured using a complete medium which includes, Dulbecco's Modified Eagle's Medium (DMEM), 10% fetal bovine serum (FBS), and 1% pen strep solution (combination of penicillin and streptomycin). The cultured cell lines were incubated in a $CO_2$ incubator at an atmospheric temperature of 37 ◦C and supplied with 5% $CO_2$.

*2.2. MTT (Methylimidazole Tetrazolium) assay*

Half maximal inhibitory concentration ($IC_{50}$) is a quantitative measure of a substance (e.g., drug) to inhibit biological processes or biological components by 50%. MTT assay is a well-known assay to determine the $IC_{50}$. The cell lines grown in monolayer were trypsinized and pelleted. The cell pellet is dissolved in a complete medium. The cells were then counted using the Trypan blue and the hemacytometer. Approximately $1 \times 10^4$ cells were seeded in 96-well plates and incubated overnight in a $CO_2$ incubator. After incubation, the old media aspired and serum-free media is added to the wells. The cells were then treated with different concentrations of Ethyl [5-(4-Chlorophenyl)-2-methyl-1H-imidazol-4-yl]-acetate ranging from 50µM to 500µM and incubated for 24 h. After the treatment period, 20ul of 5 mg/mL concentration of MTT (3 (4,5-Dimethyl-2-thiazolyl)-2,5-diphenyl-2H-tetrazolium bromide) is added to the wells and incubated for 4 h. Later, the media is removed from the wells and 200 µL of Dimethyl sulphoxide (DMSO) is added to dissolve the formazan crystals. After 30 mins of incubation, the intensity of the purple color formed is measured by an ELISA plate reader (Bio-Rad Laboratories, Hercules, CA, USA) at 595nm. MTT (RM1131) and DMSO (GRM5856) are purchased from Hi-Media Laboratories, Mumbai, India.

*2.3. Quantitative Real-time PCR (qRT-PCR):*

The A549 and NIC-H460 cells were seeded into Petri plates and grown in a complete medium. Once the growth reached 80% confluency, the cells proceeded for treatment. The $IC_{50}$ concentration of Ethyl [5-(4-Chlorophenyl)-2-methyl-1H-imidazol-4-yl]-acetate in serum-free medium is used for treatment. Whereas the control cells are maintained in a serum-free medium without Ethyl [ 5-(4-Chlorophenyl)-2-methyl-1H-imidazol-4- yl]-acetate. After the treatment period, total RNA was isolated from untreated (control) and treated A549 and NIC-H460 cell lines using TRIzol reagent (RNA isoplus). The quantity and purity of RNA is determined by BioPhotometer (Eppendorf, Hamburg, Germany). 1 µg of total RNA is taken for cDNA construction using PrimeScript RT reagent kit with manufacturer's instructions. The qRT-PCR for gene expression studies is performed in StepOnePlus real-time PCR system (Applied Biosystems, Thermos fisher scientific, MA, USA) using 2x SYBR green master mix (TB Green Premix Ex Taq II (Tli RNase H Plus). The sample preparation is done according to the instruction in the data sheet provided by the manufacturer. 0.5 µl of cDNA is used for each 10 µl reaction. The PCR condition includes initial denaturation at 94 ◦C for 5 min, followed by 40 cycles with denaturation at 94 ◦C for 30s, annealing at 55 ◦C to 60 ◦C for 30s (depending on specific gene), and melt curve stage condition's; 95 ◦C for 15s, 60 ◦C for 60s, 95 ◦C for 15s. The relative mRNA expression is calculated using the comparative threshold cycle (Ct) method (2-ΔΔCt). Glyceraldehyde 3-phosphate dehydrogenase (GAPDH) was used as an endogenous control. The list of primers used in this study is provided in (Table 1). Trizol for total RNA extraction (RNA isoplus, Cat. # 9108), PrimeScript RT reagent kit (Perfect Real Time, Cat. # RR037A) for cDNA synthesis, and syber green master mix (TB Green® Premix Ex Taq™ II (Tli RNaseH Plus, Cat. #RR820A)) for gene expression studies were purchased from Taka Bio Inc. (Japan).

**Table 1.** List of primers used in the studies.

| S. No | Gene | Primer sequence 5′-3′ | Annealing.Temp | Product Size |
|---|---|---|---|---|
| 1 | GAPDH | F′ P: ATGGGGAAGGTGAAGGTCG<br>R′ P: GGGTCATTGATGGCAACAATATC | 60 | 107 |

Preprints (www.preprints.org) | NOT PEER-REVIEWED | Posted: 7 August 2023 doi:10.20944/preprints202308.0482.v1



| | | | | |
|---|---|---|---|---|
| 2 | Keap1 | F′ P: TACTTCCGACAGTCGCTCAG<br>R′ P: GGGTTGTAACAGTCCAGGGC | 57.5 | 194 |
| 3 | Nrf2 | F′ P: CAAGTCCCAGTGTGGCATCA<br>R′ P: CCCCTGAGATGGTGACAAGG | 57.5 | 188 |
| 4 | Sirtuin 6 | F′ P: TCCCATTGTCTAGCCTCA<br>R′ P: GATGTCGGTGAATTACGC | 58.1 | 181 |
| 5 | Caspase 3 | F′ P: GCAAGTTACAGTGATGCTGTGC<br>R′ P: CCATGCCCACAGATGCCTAA | 54.9 | 166 |
| 6 | Caspase 9 | F′ P: CATCCCAGGAAGGCAACAAG<br>R′ P: GGGAAGCATGGCTAGGACTC | 54.9 | 131 |

*2.4. Western blot analysis:*

The cells grown in monolayer were treated with Ethyl [5-(4-Chlorophenyl)-2-methyl-1H-imidazol-4- yl]-acetate in serum-free medium and untreated cell lines in serum-free medium were used as control samples. After the treatment period, the cells are washed with ice-cold PBS twice and lysed with RIPA Lysis Buffer System supplemented with protease and phosphatase inhibitor cocktails. The cell lysate was centrifuged at 12,000g for 20 min at 4 °C and a supernatant containing the whole total protein was collected. The protein samples are quantified by Lowry's method. 50 µg of protein from whole protein samples are used for western blot analysis. Protein was separated by SDS-PAGE (10% and 12% gels) and separated proteins were transferred onto the nitrocellulose membrane by wet transfer. The membrane is blocked with 5% skimmed milk for 2 h. The membrane is washed with 1× TBST for 5 min for three times. After the TBST wash, the membrane is incubated overnight with specific primary antibodies at 4 ◦C. After overnight incubation membrane was washed three times with 1× TBST for 5 min each. The alkaline phosphatase-conjugated secondary antibody specific to the primary antibody was added and incubated for 4 h at 4 ◦C. Then the membrane is washed with 1× TBST for 5 min each for three times. The blots were developed with BCIP/ NBT chromogenic substrate and images were scanned. ImageJ software (National Institutes of Health, Bethesda, MD, USA) is used to measure the intensity of the bands. The protein expression in fold change is calculated after normalizing with the endogenous control Beta Actin. RIPA Lysis Buffer System (sc-24948) for protein isolation is purchased from Santa Cruz (CA, USA). Nitrocellulose Membrane (0.45µm, cat.log1620115) and Precision Plus Protein™ Kaleidoscope™ Prestained Protein Standards (#1610375) are purchased from Bio-Rad Laboratories (Hercules, California, United States). The bovine serum albumin, skimmed milk powder, and all the other fine chemical used in the SDS and western blotting are purchased from Sisco Research Laboratories Pvt. Ltd. (SRL, Maharashtra, India). All the details regarding the antibodies used in the studies are listed in Table 2.

**Table 2.** List of Antibodies used in the studies.

| S. No | Antibody | Molecular weight (kDa) | Brand | Cat. Log |
|---|---|---|---|---|
| 1 | β-Actin | 45 | Novus Biologicals | MAB8929-SP |
| 2 | Nrf2 Polyclonal Antibody | 72 | BT LAB | BT-AP06174 |
| 3 | Keap1 Polyclonal Antibody | 70 | Abbkine | ABP52949 |
| 4 | SirT6 (D8D12) Rabbit mAb | 42, 36 | Cell Signaling Technology | #12486 |
| 5 | Cleaved Caspase-3 (Asp175) (5A1E) | 17, 19 | Cell Signaling Technology | #9664 |
| 6 | caspase-3 Antibody (E-8) | 32 | Santa Cruz Biotechnology | sc-7272 |

| | | | | |
|---|---|---|---|---|
| 7 | caspase-9 Antibody (3C122) | 46, 35 | Santa Cruz Biotechnology | sc-70505 |
| 8 | Cytochrome c (A-8) | 15 | Santa Cruz Biotechnology | sc-13156 |

*2.5. Morphological Assessment:*

Approximately 1 × $10^5$ cells/well were seeded in a 6-well plate and incubated overnight for the attachment of cells. The attached cells were treated with an $IC_{50}$ concentration of Ethyl [ 5-(4-Chlorophenyl)-2-methyl-1H-imidazol-4- yl]-acetate for 24 h. The untreated cells were used as a control. After 24 h of the treatment period the cells are stained with Acridine Orange/Ethidium Bromide (AO/EtBr), DCFH-DA, Rhodamine-123, Hoechst and Propidium iodide (PI) dyes for 10 min. After incubation the cells were washed with PBS and morphological changes were captured using an inverted fluorescence microscope (Floid cell imaging station, USA) with 20× magnification.

*2.6. Assessment of the Antioxidant and Radical Scavenging Activity:*

Biochemical analysis of Enzymatic antioxidants such as Catalases and Glutathione Peroxidases (GPX), non-enzymatic antioxidant GSH, % Radical Scavenging Activity (%RSA) are performed with cell homogenate of control (untreated) and Ethyl [5-(4-Chlorophenyl)-2-methyl-1H-imidazol-4- yl]-acetate treated. The cells grown in a monolayer were treated with Ethyl [5-(4-Chlorophenyl)-2-methyl-1H-imidazol-4-yl]-acetate and untreated cells are used as control. After treatment, the cells were lysed with RIPA lysis buffer. Then Centrifuge sample for 20 minutes at 4°C at 12,000 rpm. The supernatant is collected and used for antioxidant studies.

To determine the GSH levels, 10% homogenate is added to water and 10%TCA for deproteination. the content is then centrifuged and the supernatant is collected. 1 ml of supernatant is added to 4 ml of 0.3M phosphate solution and 0.5 ml of DTNB (2mg /5ml) (5-5'- dithiobis [2-nitrobenzoic acid]). DTNB reacts with GSH to form a yellow color chromophore, 5- thionitrobenzoic acid (TNB) with absorbance maxima at 412 nm. After 5mins of incubation at room temperature, the absorbance at 412 nm is recorded using a UV-Visible spectrophotometer. Except for the cell homogenate, all the other reagents in the reaction are used as blank. The GPx activity assay is performed by the method of Paglia and Valentine (1967) [30]. The reaction mixture contains 0.4 ml of 0.4M phosphate buffer (pH 7), 0.1 ml sodium azide (16mM), 0.2 ml reduced glutathione (4mM), 0.1 ml of H2O2 (2.5 mM), and 0.2 ml of homogenate. The mixture was incubated at room temperature for 0, 90 sec, and 180 sec. The reaction was arrested by adding 0.5ml of 10% TCA and the tubes were centrifuged at 2,000 rpm. To 1ml of the supernatant, 3ml of phosphate disodium hydrogen phosphate (0.3mM) and 1ml of DTNB (0.04%) is added. The color developed was read in photometric mode at 412 nm. The reaction mixer except the cell homogenate is considered as blank. Catalase activity is determined by the rate of decomposition of H2O2 (Aebi, 1984) [31]. To 0.1ml of homogenate, 1ml of phosphate buffer (50mM, pH 7) and 0.5ml of H2O2 (20mM) were added and incubated for 0 min, 30 min, and 60 min. After the incubation, the reaction was stopped by adding 2 ml of potassium dichromate. The results were calculated from the extension coefficient of $H_2O_2$ at 240nm. The reaction mixer without a sample is taken as blank. DPPH assay (2,2-Diphenyl-1-picrylhydrazyl) is performed to determine the %RSA by Mensor LL et al. protocol [32]. DPPH reacts with antioxidants and gets converted to a reduced form of DPPH indicated by the change of color from deep violet (DPPH) to light yellow (DPPH). The assay is performed by adding 3ml of ethanol, 0.5ml of the 10% cell homogenate, and 0.3ml of freshly prepared DPPH (0.5mM) solution. 3.3ml of ethanol. The samples are incubated for 100 mins and the change in color was read at 517nm using a UV-VIS spectrophotometer. 3.3 ml of ethanol and 0.5 ml of sample is used as blank, 3.5 ml of ethanol and 0.3ml DPPH is used as control %RSA is calculated using the following formula:

% RSA = 100 — [(Sample Abs — Blank Abs)/Control Abs X 100]

*2.7. Statistical analysis:*

Preprints (www.preprints.org) | NOT PEER-REVIEWED | Posted: 7 August 2023 doi:10.20944/preprints202308.0482.v1



The graphical presentation of the data in this study is from biological replicates and presented as the mean ± SD done using ordinary one-way ANOVA with Tukey's multiple comparisons test by GraphPad Prism software (version 9.4.0, CA, USA). The Significance is represented as *p < .05 and **p < .01, ***p < .001 and ****p < .0001.

**3. Results:**

*3.1. Cytotoxicity effect of Ethyl [5-(4- Chlorophenyl)-2-methyl-1H-imidazol-4-yl}-acetate*

The cytotoxicity of Imidazole and its derivative Ethyl [5-(4- Chlorophenyl)-2-methyl-1H-imidazol-4-yl}-acetate is determined in NSCLC cell lines A549 and NIC-H460 using MTT assay. The cells were treated with imidazole derivative ranging from 0 µM to 500 µM concentration for 24 h. The cell viability is decreased gradually with an increase in concentration. The half maximal inhibitory concentration ($IC_{50}$) was found to be 250 µM in A549 and 300 µM in the NIC-H460 cell line **(Figure 1. A, B)**.

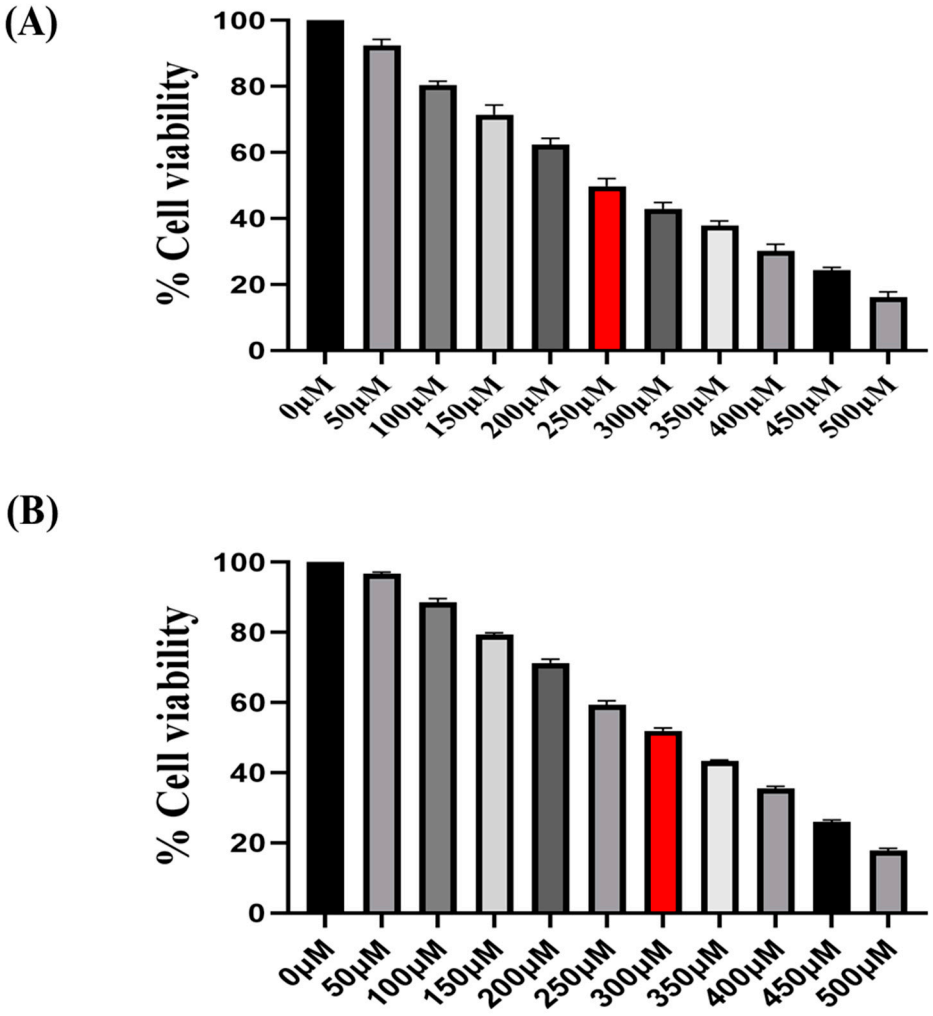


**Figure 1.** Illustrates the cytotoxicity activity of Ethyl [5-(4-Chlorophenyl)-2-methyl-1H-imidazol-4-yl}-acetate in A549 **(A)** and NIC-H460 cell lines **(B)**.

*3.2. In-vitro studies on effect of Ethyl [ 5-(4- Chlorophenyl)-2-methyl-1H-imidazol-4-yl}-acetate on Sirtuin 6:*

The in-vitro analysis of SIRT6 expression in NSCLC cell lines, specifically A549 and NIC-H460, was conducted using Ethyl [5-(4-Chlorophenyl)-2-methyl-1H-imidazol-4-yl}-acetate treated and

Preprints (www.preprints.org) | NOT PEER-REVIEWED | Posted: 7 August 2023 doi:10.20944/preprints202308.0482.v1



untreated samples.The results of gene and protein expression studies revealed that SIRT6 expression was decreased in both A549 and NIC-H460 cell lines when treated with Ethyl [5-(4-Chlorophenyl)-2-methyl-1H-imidazol-4-yl}-acetate **(Figure 2. A, B)**. This indicates that Ethyl [5-(4-Chlorophenyl)-2-methyl-1H-imidazol-4-yl}-acetate has an inhibitory effect on SIRT6.

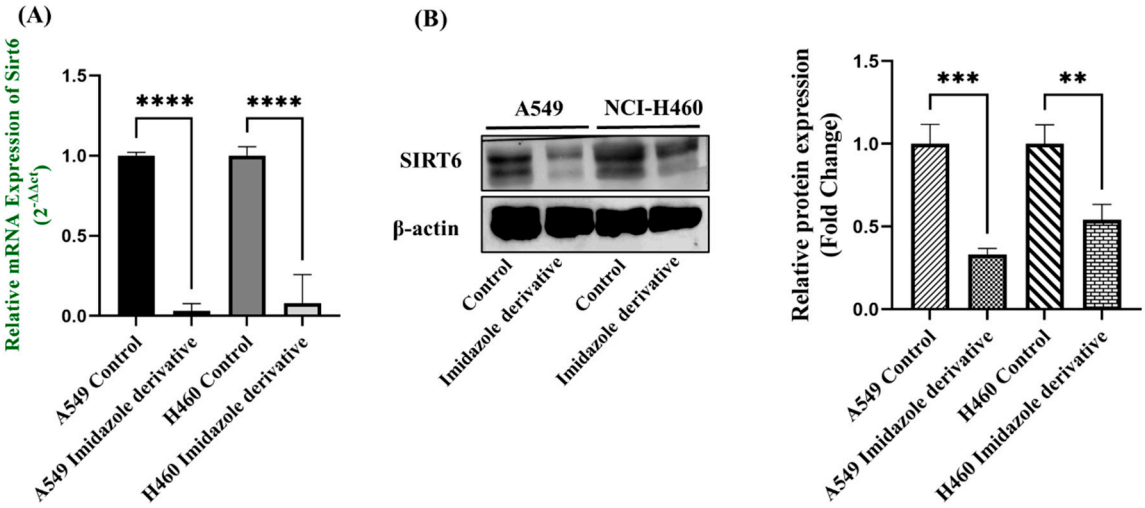


**Figure 2.** SIRT6 expression in A549 and NIC-H460 NSCLC cell lines: **(A)** Represents the qRT-PCR analysis and **(B)** represents the Western blot analysis. GAPDH for gene expression and β-Actin for protein expression was used as an internal control for normalization. (Data represent mean values ± SD. *$p < 0.05$, **$p < 0.01$ and ****$p < 0.0001$).

*3.3. SIRT6 inhibition affects anti-oxidant systems:*

We performed a biochemical assay to check the fate of anti-oxidant molecules upon inhibition of SIRT6 in NSCLC cell lines. We estimated the levels of both enzymatic (GPx, and Catalase) and non-enzymatic anti-oxidant molecules (GSH). GSH, GPx, and Catalase levels were reduced in Ethyl [5-(4-Chlorophenyl)-2-methyl-1H-imidazol-4-yl}-acetate-treated cells **(Figure 3. A, B, C)**. Further, the anti-oxidant activity is determined by the free radical scavenging activity of DPPH **(Figure 3. D)**. The % radical scavenging activity is deprived in cells treated with imidazole derivative as compared with untreated cells. Thus, the results from anti-oxidant assays confirm SIRT6 inhibition impacts on low levels of anti-oxidant molecules thereby blocking the adaptation of cancer cells to oxidative stress.

Preprints (www.preprints.org) | NOT PEER-REVIEWED | Posted: 7 August 2023 doi:10.20944/preprints202308.0482.v1



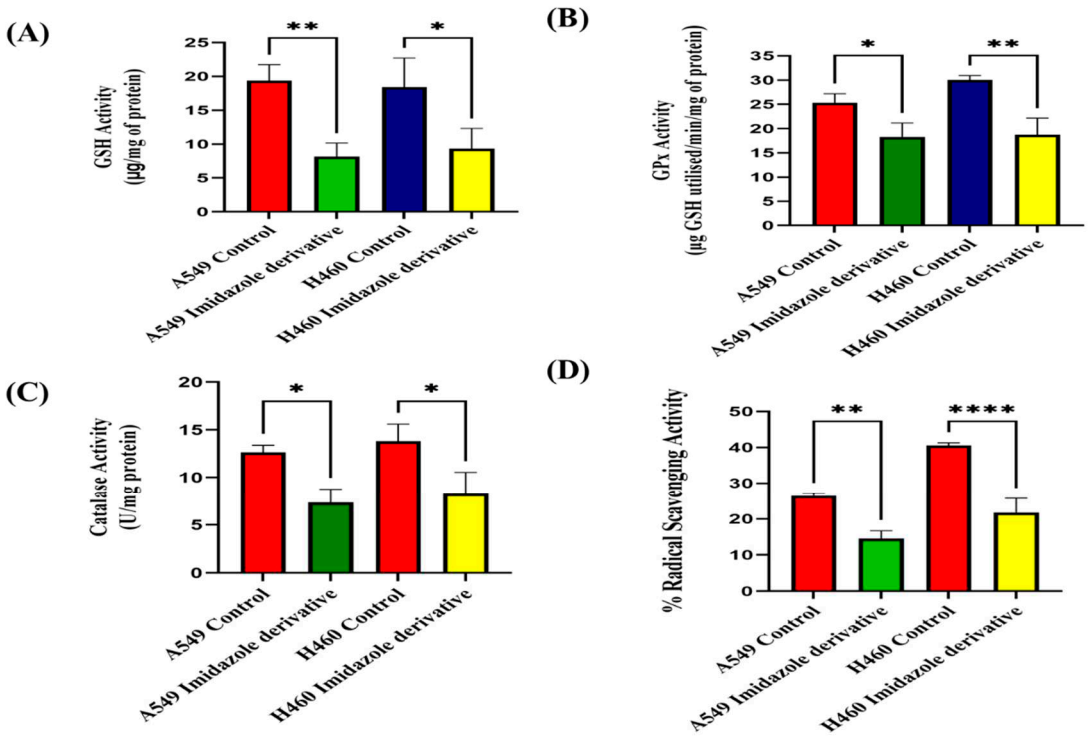


**Figure 3.** Effect of imidazole ester on anti-oxidant regulators **(A)** GSH Activity, **(B)** GPx Activity, **(C)** Catalase Activity, and **(D)** % Radical Scavenging Activity in A549 and NIC-H460 cell lines. (Data represent mean values ± SD. *p < 0.05, **p < 0.01, ***p < 0.001 and ****p < 0.0001).

*3.4. Oxidative stress impact on apoptosis:*

The imbalance between the reactive oxygen species (ROS) and anti-oxidant mechanisms causes the accumulation of ROS leading to Oxidative stress. The accumulation of ROS above the threshold level destruct mitochondria. Since mitochondria are majorly involved in the intrinsic apoptosis pathway. Hence, we studied the downstream regulator of intrinsic apoptosis pathways such as Cytochrome -c (Cyt-c), Caspase 9, and Caspase 3. Elevated levels of Cyt-c were observed in Ethyl [5-(4- Chlorophenyl)-2-methyl-1H-imidazol-4-yl}-acetate treated cell lines compared to untreated cells **(Figure 4.)**. Further, we studied the gene and protein expression of caspases 9 and caspase 3 involved in the intrinsic apoptosis pathway. The gene expression of caspase 9 was upregulated, the protein expression of procaspase 9 is downregulated and active caspase 9 showed increased expression **(Figure 5. A, B, C)**. Caspase 3 gene expression was increased, the protein expression of procaspase 3 decreased, and active caspase 3 increased in NSCLC cell lines **(Figure 6. A, B, C)**. These results confirm the involvement of oxidative stress in mitochondrial damage-mediated apoptosis.

Preprints (www.preprints.org) | NOT PEER-REVIEWED | Posted: 7 August 2023 doi:10.20944/preprints202308.0482.v1



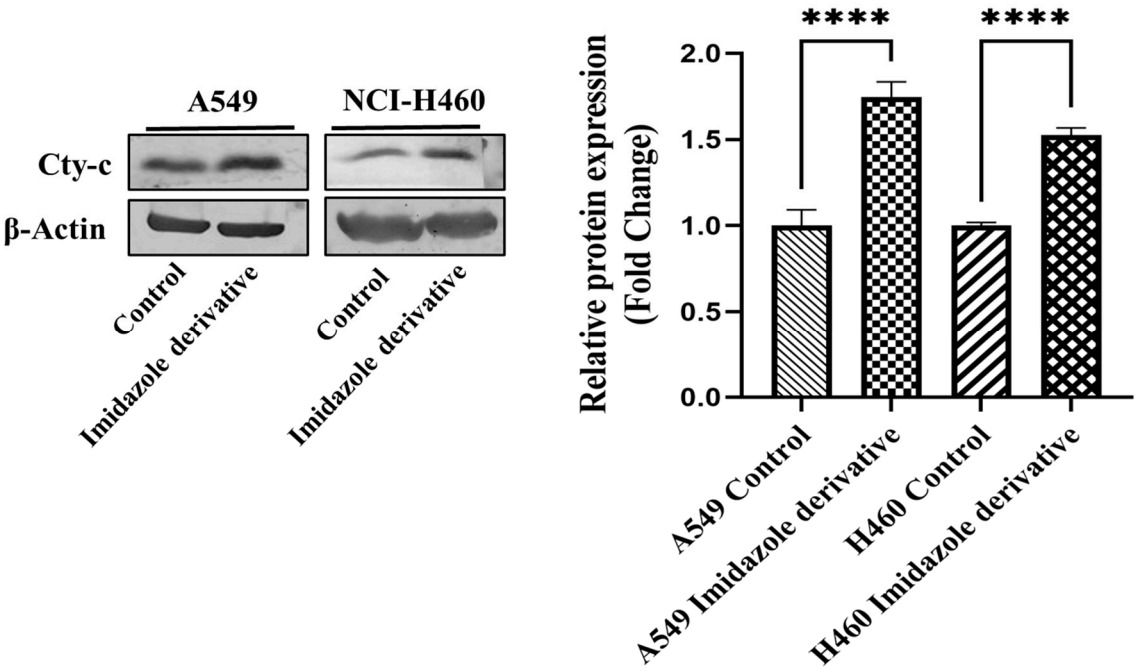


**Figure 4. S**hows the protein expression of Cytochrome-c (Cyt-c) in NSCLC cell lines A549 and NIC-H460. GAPDH for gene expression and β-Actin for protein expression was used as an internal control for normalization. (Data represent mean values ± SD. ****$p < 0.0001$).

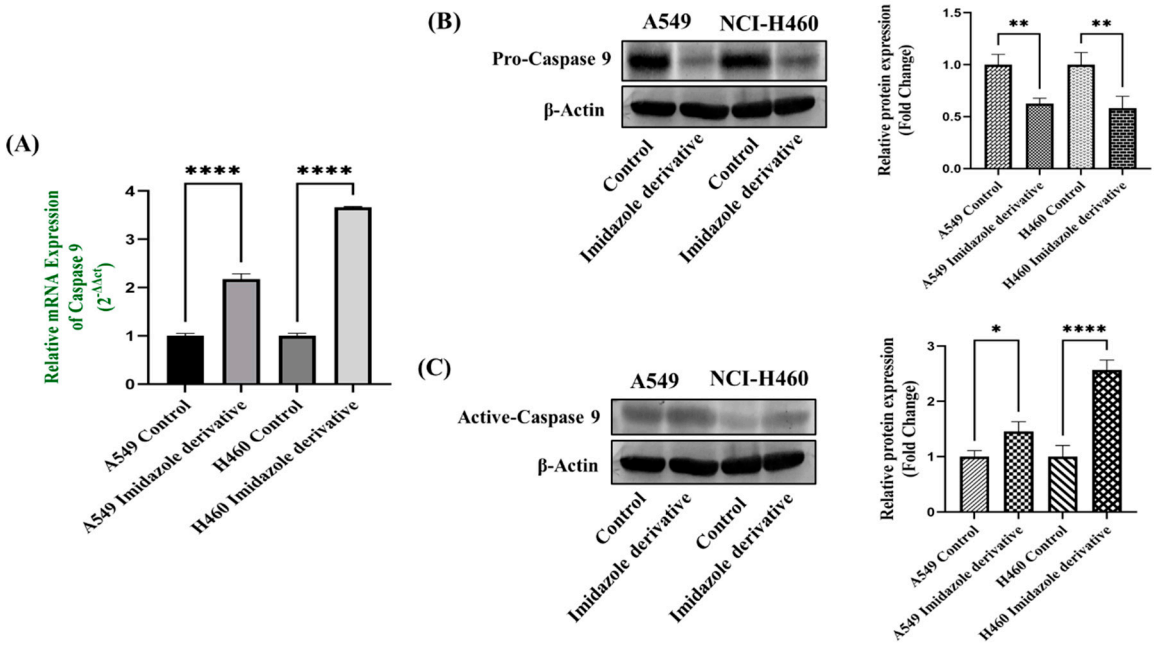


**Figure 5.** Represents the Caspase 9 **(A)** gene expression, pro-caspase 9 **(B),** and Active-caspase 9 **(C)** Protein expression in A549 and NIC-H460 cell lines. GAPDH for gene expression and β-Actin for protein expression was used as an internal control for normalization. (Data represent mean values ± SD. *$p < 0.05$, **$p < 0.01$ and ****$p < 0.0001$).

Preprints (www.preprints.org) | NOT PEER-REVIEWED | Posted: 7 August 2023 doi:10.20944/preprints202308.0482.v1



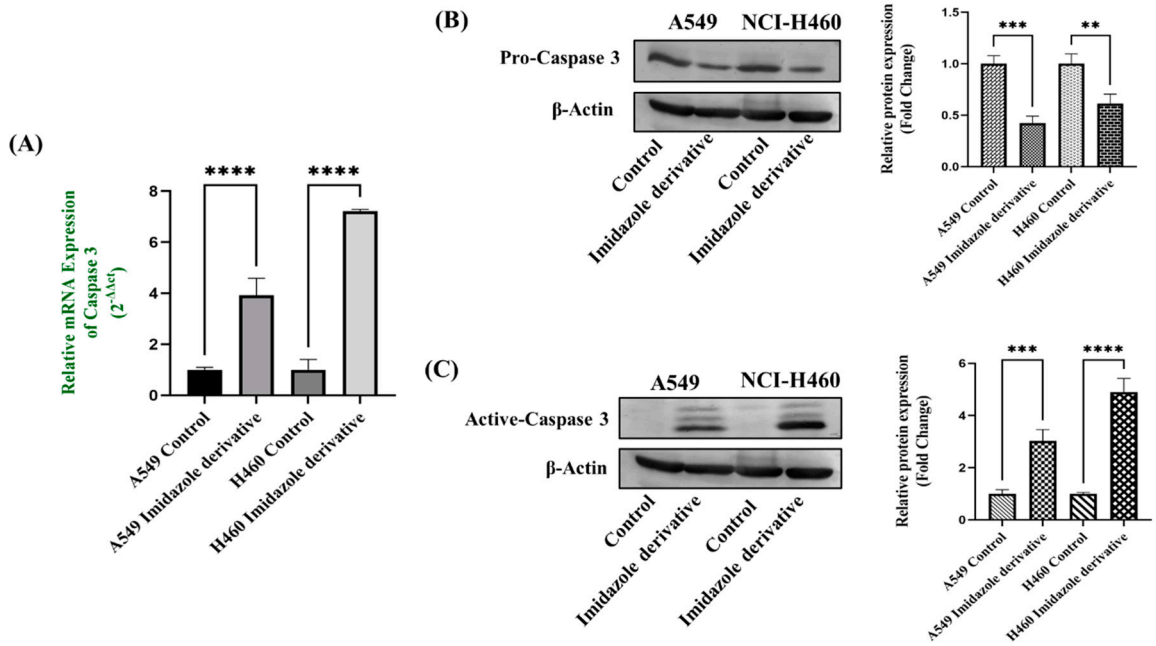


**Figure 6.** Gene expression of Caspase 3 (5a), Protein expression of pro-caspase 3 (5b), and Active-caspase 3 (5c) in A549 and NIC-H460 cell lines. GAPDH for gene expression and β-Actin for protein expression was used as an internal control for normalization. (Data represent mean values ± SD.**$p < 0.01$, ***$p < 0.001$ and ****$p < 0.0001$).

*3.5. Morphological changes during SIRT6 inhibition in NSCLC cell lines:*

We initially performed AO/EB staining to examine the axis of apoptosis upon SIRT6 inhibition. The green fluorescence represents healthy viable cells with intact membranes, orange fluorescence represents early apoptotic cells and red fluorescence indicates late apoptosis. Propidium iodide (PI) dye selectively binds to DNA by intercalating between the base pairs. As PI is impermeable to live cells with intact plasma membranes, it can stain dead or damaged cells. The results show that the live cells image appears black without any red fluorescence and the image of damaged and dead cells appeared red due to emission of red fluorescence. Mitochondrial Membrane Potential ($\Delta\Psi m$) is assessed by using Rhodamine 123 dye. Rhodamine 123 dye is highly sensitive to changes in mitochondrial membrane potential. The results from Rhodamine 123 show that healthy cells with intact mitochondria have an intense emission of fluorescence. Whereas cells with mitochondrial damage as reduced fluorescence emission. DCFH-DA staining is performed to determine whether the SIRT6 inhibition generates ROS. The DCFH-DA gets oxidized to the fluorescent compound called 2',7'-dichlorofluorescein (DCF). DCF emits a green fluorescence and the intensity of the fluorescence is proportional to the level of ROS present in the cells. The results confirm that Ethyl [5-(4-Chlorophenyl)-2-methyl-1H-imidazol-4-yl}-acetate treated cells have emitted high-intensity of green fluorescence compared to untreated cells. Hoechst dyes are often used to stain the cell nuclei to visualize the nuclear morphology and damage of DNA within cells. Hoechst staining emits blue fluorescence when they bind to DNA. The results show high intense blue fluorescence emission in Ethyl [5-(4- Chlorophenyl)-2-methyl-1H-imidazol-4-yl}-acetate treatment **(Figure 7.)**.

Preprints (www.preprints.org) | NOT PEER-REVIEWED | Posted: 7 August 2023 doi:10.20944/preprints202308.0482.v1



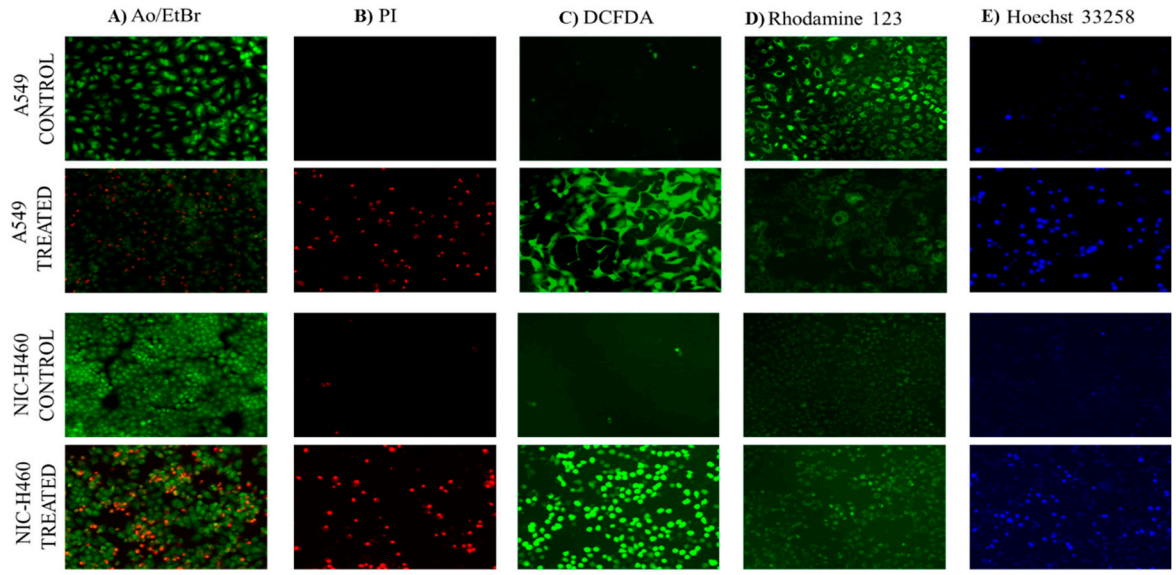


**Figure 7.** Microscopical staining in NSCLC cells: Control (untreated) and Imidazole derivative treated A549 and NCI-H460 cells stained by AO/EB **(A)**, Propidium iodide **(B)**, DCFDA **(C)**, Rhodamine 123 **(D)** and Hoechst 33258 (E). Images were captured using a Fluorescent microscope (**Scale Bar - 125 µM**).

*3.6. Nrf2/Keap1 regulation upon SIRT6 inhibition:*

Nrf2/Keap1 signaling is involved in the activation anti-oxidant mechanism to prevent oxidative stress, thereby protecting the cells from death. Nrf2 is majorly involved in the activation of these mechanisms. Whereas Keap1 prevents the interaction of Nrf2 with anti-oxidant systems. Since SIRT6 is found to be very well involved in the regulation of Nrf2, we studied the expression of Nrf2/Keap1 by inhibiting SIRT6 with Ethyl [ 5-(4- Chlorophenyl)-2-methyl-1H-imidazol-4-yl}-acetate in NSCLC cell lines. The expression of Nrf2, a key regulator of oxidative stress was downregulated, whereas Keap1 was upregulated in cells treated with Ethyl [ 5-(4- Chlorophenyl)-2-methyl-1H-imidazol-4-yl}-acetate. Further, protein expression studies are performed to know the Nrf2 and Keap1 expression at the protein level. The results were well correlated with gene expression with downregulation of Nrf2 and upregulation of Keap1 in cells treated with Ethyl [5-(4- Chlorophenyl)-2-methyl-1H-imidazol-4-yl}-acetate clearly reveals that SIRT6 inhibition alters the expression of Nrf2/Keap1 signaling in NSCLC cells **(Figure 8. A, B, C, D)**.

Preprints (www.preprints.org) | NOT PEER-REVIEWED | Posted: 7 August 2023 doi:10.20944/preprints202308.0482.v1



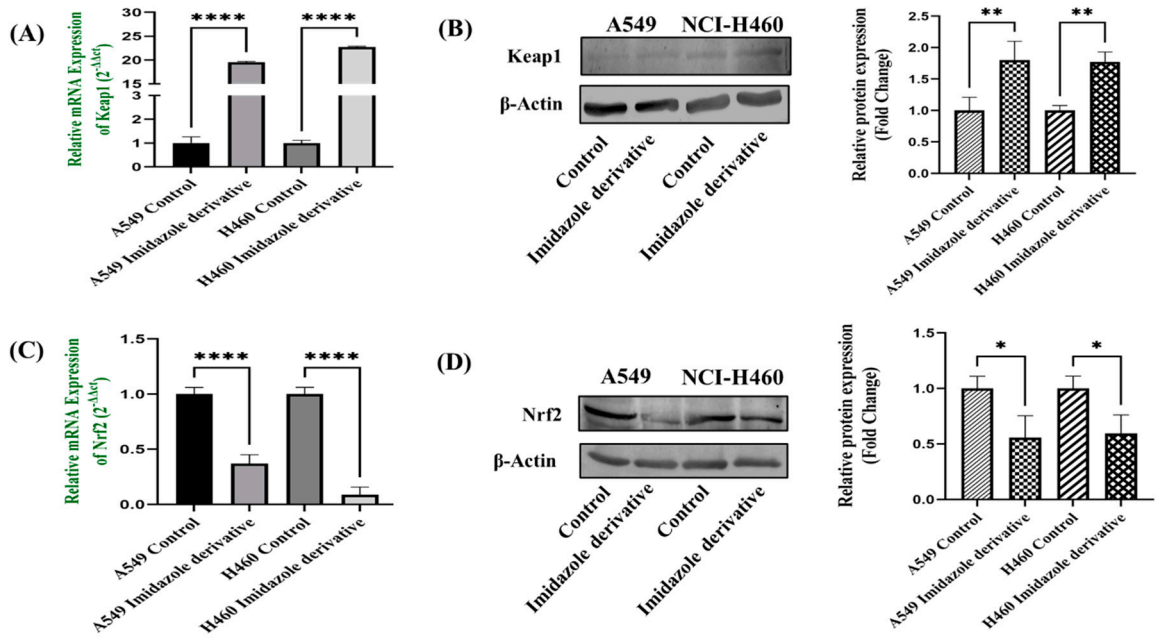


**Figure 8.** Gene and protein expression of Keap1 and NRf2 in A549 and NIC-H460 NSCLC cell lines: (a) qRT-PCR and (b) Western blot analysis of keap1, (c) qRT-PCR and (d) Western blot analysis of Nrf2. GAPDH for gene expression and β-Actin for protein expression was used as an internal control for normalization. (Data represent mean values ± SD. *$p < 0.05$, **$p < 0.01$ and ****$p < 0.0001$).

## 4. Discussion

Epigenetic dysregulation is a common mechanism in the onset of cancer [33]. Gene regulation is often maintained by the epigenetic modifications associated with DNA methylation and histone methylation/acetylation. The role of chromatin-modifying enzymes particularly sirtuins were extensively studied in the initiation and progression of cancer. The overexpression of SIRT6 possesses oncogenic effects in the development and progression of tumor cells and thus has become a target for epigenetic therapy. Numerous studies were in progress to identify novel compounds targeting SIRT6 which may provide a new approach in the development of epigenetic therapy. The discovery of imidazole in the 1840s prompted extensive research in drug discovery, focusing on imidazole-based compounds [24]. Imidazole, an important heterocyclic compound and a core component of FDA-approved drugs, has demonstrated favorable activities in practical applications. It serves as a fundamental building block in numerous natural and synthetic bioactive compounds. The imidazole scaffold offers advantages in binding with various receptors, proteins, and enzymes [34]. Imidazole exhibits diverse pharmaceutical activities, including anticancer, antiviral, antibacterial, antifungal, antihistaminic, anti-inflammatory, and other medicinal properties. Notably, imidazole has proven to be an effective anticancer agent. Several imidazole derivatives, such as nilotinib, tipifarnib, zoledronic acid, mercaptopurine, dacarbazine, and temozolomide, are currently employed in the treatment of various cancers. Due to its extensive pharmacological properties, researchers have explored derivatives of imidazole to enhance efficiency and reduce side effects, aiming to overcome the limitations of currently available clinical drugs [24].

In the present study, we explored the modulatory effect of imidazole derivative Ethyl [5-(4-Chlorophenyl)-2-methyl-1H-imidazol-4-yl}-acetate, a SIRT6 inhibitor on Nrf2/Keap1 signaling. This compound possesses various functional groups including an Ethyl group, Acetate group, Chlorophenyl group, and Methyl group, with imidazole serving as the structural backbone. The presence of these functional groups might benefit in terms of improved bioavailability and cell membrane permeability, enhanced drug stability and solubility, increased lipophilicity and metabolic stability in the compound, potentially augmenting the compound's binding affinity and

 doi:10.20944/preprints202308.0482.v1



selectivity, fitting of the molecule into the target binding site. At first, we performed the MTT assay to determine the effect of Ethyl [5-(4- Chlorophenyl)-2-methyl-1H-imidazol-4-yl}-acetate on the proliferation of NSCLC cell lines A549 and H460. The findings reveal that the imidazole derivative significantly diminishes the viability of A549 at an $IC_{50}$ concentration of 250 μM and 300 μM in NIC-H460 cell lines.

Further, we investigated the impact of imidazole derivative on oxidative stress mechanisms using the ic 50 values. Redox cellular homeostasis is a balanced ratio of the rate and quantity of oxidant generation to the rate of oxidant detoxification. The imbalance between oxidant generation and oxidant detoxification results in Oxidative stress [35]. Managing oxidative stress involves maintaining a balance between ROS production and antioxidant defense systems [36]. Cancer cells exhibit a higher rate of ROS generation and experience a modified redox environment compared to normal cells [37]. ROS includes free radicals such as hydroxyl (HO*) and superoxide (O2 *) and non-radical molecule like hydrogen peroxide ($H_2O_2$) [36]. Antioxidants are the molecules precisely regulate redox balance. These anti-oxidant molecules exist in enzymatic and non-enzymatic forms, the enzymatic anti-oxidants act by breaking down and removal of free radicals. Whereas non-enzymatic anti-oxidants act by interfering with radical chain reactions [38]. The enzymatic antioxidant defense systems are regulated by superoxide dismutase (SOD), Glutathione peroxidase (GPx), and Catalase (CAT). Superoxide dismutase (SODs) act by dismutation of two molecules of O2− into hydrogen peroxide (H2O2) and molecular oxygen (O2) [39]. Glutathione peroxidases (GPXs) catalyze the reduction of H2O2 and lipid hydroperoxides by using reduced glutathione (GSH) and Catalase (CAT) too involved in the conversion of H2O2 to water [40]. Ascorbic acid (vitamin C), α-tocopherol (vitamin E), glutathione (GSH), and β-carotene are the non-enzymatic anti-oxidant molecules [39]. GSH is a tripeptide of cysteine, glycine, and glutamate amino acids and serves as a cofactor for several antioxidant enzymes, including glutathione peroxidase (GPx) and regeneration of other essential antioxidants like vitamin C (ascorbic acid) and vitamin E (α-tocopherol) [41]. The morphological examination of ROS by DCFH-DA dye, biochemical analysis of enzymatic anti-oxidant such as Glutathione peroxidases (GPXs) and Catalase (CAT), non-enzymatic anti-oxidant molecules Glutathione (GSH) in Imidazole derivative treated A549 and NIC-H460 supported the ROS generation and accumulation in NSCLC cell lines. Further, the decreased levels of the important anti-oxidant molecules support the decrease in free radical scavenging activity conformed by the % Radical Scavenging activity assay.

We previously reported that knockdown of SIRT6 inhibits growth and induces cell cycle arrest, and apoptosis in NSCLC apoptosis [20]. We were eager to investigate whether our imidazole derivative-based SIRT inhibitor can able to induce apoptosis in NSCLC cells. We focused on the molecular expression studies of key regulators that mediate the intrinsic apoptosis pathway such as cytochrome-c, caspases 9, and caspase 3. We found the release of cytochrome-c and its accumulation in the cytosol which initiated the caspase 9 activation, caspase 9 in turn activate the caspase 3 the end effector molecule of the apoptosis cascade, ultimately leading to cell death. The protein expression results confirm that the Cytochrome-c is high in imidazole derivative treated cells compared to control cells. Further, gene expression studies confirm the increase in expression of caspase 9 and caspase 3 and the protein expression studies show the decrease in expression of pro-caspase 9 and pro-caspase- 3, increased expression of active caspase-9 and active caspase 3. Thus, the results from morphological studies and molecular expression studies confirm the significant role of imidazole derivative in apoptosis-induced cell death of A549 and NIC-H460 cell lines.

Reactive oxygen species (ROS), levels below and above the threshold range have the opposite impact on cancer. The ROS levels below the threshold range contribute to the onset, advancement, angiogenesis, and metastasis of tumors by instigating DNA mutations, genomic instability, and abnormal pro-tumorigenic signaling. Various cancer types such as breast, lung, liver, and others have shown a correlation between ROS-induced cell proliferation [37,40]. Conversely, when ROS levels exceed the threshold, they become detrimental to cancer cells, triggering oxidative stress-induced signals that result in cell cycle arrest, senescence, and apoptotic cell death [42]. This was quite evident from our studies of morphological assessment of apoptosis in NSCLC cell lines. Propidium iodide

(PI) stain is used to assess the live and dead cells. PI is not permeant to viable cells, so the viable cells appear black due to no red fluorescence, whereas dead cells appear red due to PI entry into damaged cells and stain DNA by intercalating between the bases with little or no sequence preference. Further, AO/ETBR confirms the occurrence of cell death at different stages such as early apoptosis and late apoptosis. The viable cells showed uniformly distributed green color with organized chromatin structures. In apoptotic cells, the chromatin is condensed or fragmented, with yellowish-green fluorescence representing early apoptosis and orange nuclear ethidium bromide indicating late apoptosis. The Necrotic death is indicated by uneven orange-red fluorescence. Hoechst 33258 dye is employed to examine the condensation and fragmentation of nuclei, which are characteristics of apoptosis. The results revealed that the control cells are uniformly stained and have regular, round-shaped nuclei. The treated cells have become highly condensed and appear as bright, compacted spots. The nuclei show signs of fragmentation, with the multi-smaller nuclei, also called as apoptotic bodies. Mitochondria is a key regulator of apoptosis, in particular intrinsic apoptosis pathway which includes a cascade of events such as change in mitochondrial membrane potential, cytochrome-c release, and activation of caspase molecules [43]. The Rhodamine 123 green-fluorescent dye measure changes in mitochondrial membrane potential. The results show the control cells with intact mitochondria accumulate Rhodamine 123, leading to strong fluorescence. Whereas the treated cells have reduced Rhodamine 123 uptake and lower fluorescence confirming the decrease of mitochondrial membrane potential. All together the morphological studies confirm the role of the imidazole derivative in ROS generation and accumulation, damage of mitochondrial membrane potential, and apoptosis cell death.

Since the nuclear factor erythroid-2-related factor 2/ Kelch-like ECH-associated protein 1 (NRF2/KEAP1) is reported to be a major regulator of cellular homeostasis and SIRT6 is very well involved in the regulation of NRF2. We investigated the impact of SIRT6 inhibition on Nrf2/Keap1 signaling. Nrf2, a crucial transcription factor that regulates cytoprotective responses against xenobiotic/electrophilic and oxidative stress, plays a significant role in cancer development, progression, and resistance [44]. Nrf2 exerts its influence through the Antioxidant Responsive Element (ARE) found in the 5'-upstream regulatory regions of most cytoprotective genes, which allows it to modulate oxidative stress [45]. The regulation of Nrf2 is controlled by its suppressor protein, Keap1, acting as an on/off switch in response to redox stimuli. Under normal redox conditions, Keap1 binds to and retains Nrf2 in the cytosol. Keap1 also functions as a substrate adapter for the Cullin 3 (CUL3)-containing E3-ligase complex, leading to the ubiquitination of NRF2 and its subsequent degradation by the 26S proteasome [46]. However, during oxidative stress, specific cysteine residues in Keap1 act as sensors and undergo conformational changes that prevent Keap1 from binding to Nrf2. Consequently, Nrf2 translocates to the nucleus, where it partners with small Maf or other nuclear proteins to bind to ARE, thereby activating genes involved in the antioxidant mechanism [47]. The results of our biochemical analysis of anti-oxidants GPx, Catalase, and GSH, and morphological studies of ROS generation confirm the role of Nrf2/Keap1 signaling. The accumulation of Nrf2 in cancer cells and its cytoprotective role in cancer can be attributed to several factors. Firstly, somatic mutations in NRF2, KEAP1, or CUL3 have been reported. Secondly, Keap1 downregulation can occur through epigenetic mechanisms. Thirdly, the interaction of p62/Sqstm1 and p21 with Keap1 can influence Nrf2 levels. Lastly, on cometabolites can modify Keap1 cysteine residues [48]. Our data shows that the Nrf2 is downregulated, whereas the Keap1 is upregulated at gene and protein expression levels. The gene and protein expression data of Nrf2 and Keap1, the key components of Nrf2/Keap1 signaling conform the imidazole derivative induced apoptosis through oxidative stress.

## 5. Conclusion

In conclusion, the overall findings of our work indicate that the imidazole derivative Ethyl [5-(4-Chlorophenyl)-2-methyl-1H-imidazol-4-yl}-acetate a potential SIRT6 inhibitor affects the Nrf2/Keap1 signaling pathway which holds key control in regulating oxidative stress and responsible for cancer progression. Consequently, interrupting Nrf2/Keap1 signaling pathway disrupts the

antioxidant mechanisms, causing an accumulation of reactive oxygen species (ROS) and resulting in oxidative stress. Moreover, oxidative stress-induced mitochondrial damage triggers the activation of the intrinsic apoptosis pathway in A549 and NIC-H460 cell lines. Hence targeting SIRT6 might be a new promising cancer treatment strategy to evade Nrf2/Keap1-powered cellular rescue pathways.

**Author Contributions:** Conceptualization: R.V., D.U.M.R., and T.R. Study Design and execution: D.U.M.R. Data analysis and summary: S.A.G., N.A.A., S.B.D., A.A.A., M.S. Writing original draft: D.U.M.R., R.V. Writing review& editing: D.U.M.R., R.V.

**Acknowledgments:** The authors acknowledge the RUSA-2.0 (Biological Sciences, BDU), DST-PURSE Phase II, and, DST-FIST, Government of India for their support in providing funds for the improvement of instrumentation facilities in our department. The authors would also like to acknowledge a research grant from the Indian Council of Medical Research (ICMR), New Delhi, India. (Ref. No: 52/13/2020-BIO-BMS and Ref. No: VIR/ COVID-19/6/2021/ECD-I). We wish to acknowledge Dr. K. Srinivasan, Professor, School of Chemistry, Bharathidasan University for providing the Imidazole derivative which was used in the present study; Dr. Mahesh Kandasamy, UGC-Assistant Professor, Department of Animal Science, Bharathidasan University for giving suggestions in framing the work.

**Ethics approval and consent to participate:** Not applicable.

**Consent for publication:** All authors consented to publish this study.

**Availability of data and materials:** Sets of data or summaries generated during the present study are available from the corresponding author upon reasonable request.

**Competing interests:** The authors declare no competing interests.

Compliance with Ethical Standards.

**Disclosure of potential conflicts of interest:** The authors declare that there is no conflict of interest.

**Research involving human participants and/or animals:** Not applicable.

**Informed consent:** Not applicable.

## Abbreviation

NSCLC, Non-small cell lung cancer; A549, Adenocarcinoma; NIC-H460, ; HDAC, Histone deacetylase; HDACi, Histone deacetylase inhibitor; Nrf2, Nuclear factor erythroid 2-related factor 2 (NRF2); Keap1, Kelch-like ECH-associated protein 1; SIRT6, Sirtuin 6; ROS, Reactive oxygen species; %RSA, % Radical Scavenging Activity; GSH, Glutathione; GPx, Glutathione peroxidases; CAT, Catalase; PI, Propidium iodide; AO, Acridine orange; ETBR, Ethidium Bromide; ARE, Antioxidant Responsive Element; DCFH-DA, 2 2′,7′-dichlorofluorescin; DTNB, 5,5′-dithiobis-(2-nitrobenzoic acid) (Ellman's reagent); DPPH, 2,2-diphenylpicrylhydrazyl; Cyt-c, Cytochrome-c.

## References

1. Alduais Y, Zhang H, Fan F, Chen J, Chen B. Non-small cell lung cancer (NSCLC): A review of risk factors, diagnosis, and treatment. Medicine. 2023 Feb 22;102(8):e32899.
2. Tossetta G, Marzioni D. Targeting the NRF2/KEAP1 pathway in cervical and endometrial cancers. European Journal of Pharmacology. 2023 Jan 12:175503.
3. Ma Q. Role of nrf2 in oxidative stress and toxicity. Annual review of pharmacology and toxicology. 2013 Jan 6;53:401-26.
4. Tossetta G, Fantone S, Marzioni D, Mazzucchelli R. Role of Natural and Synthetic Compounds in Modulating NRF2/KEAP1 Signaling Pathway in Prostate Cancer. Cancers. 2023 Jun 2;15(11):3037.
5. Fuchs-Tarlovsky V. Role of antioxidants in cancer therapy. Nutrition. 2013 Jan 1;29(1):15-21.
6. Wu S, Lu H, Bai Y. Nrf2 in cancers: A double-edged sword. Cancer medicine. 2019 May;8(5):2252-67.
7. Schmidt H, Hangmann J, Shams I, Avivi A, Hankeln T. Molecular evolution of antioxidant and hypoxia response in long-lived, cancer-resistant blind mole rats: The Nrf2–Keap1 pathway. Gene. 2016 Feb 15;577(2):293-8.
8. Kobayashi A, Kang MI, Watai Y, Tong KI, Shibata T, Uchida K, Yamamoto M. Oxidative and electrophilic stresses activate Nrf2 through inhibition of ubiquitination activity of Keap1. Molecular and cellular biology. 2006 Jan 1;26(1):221-9.

9. Leung CH, Zhang JT, Yang GJ, Liu H, Han QB, Ma DL. Emerging Screening Approaches in the development of Nrf2–Keap1 protein–protein interaction inhibitors. International Journal of Molecular Sciences. 2019 Sep 10;20(18):4445.
10. Yoo NJ, Kim HR, Kim YR, An CH, Lee SH. Somatic mutations of the KEAP1 gene in common solid cancers. Histopathology. 2012 May;60(6):943-52.
11. DeBlasi JM, DeNicola GM. Dissecting the crosstalk between NRF2 signaling and metabolic processes in cancer. Cancers. 2020 Oct 17;12(10):3023.
12. Lu K, Alcivar AL, Ma J, Foo TK, Zywea S, Mahdi A, Huo Y, Kensler TW, Gatza ML, Xia B. NRF2 induction supporting breast cancer cell survival is enabled by oxidative stress–induced DPP3–KEAP1 interaction. Cancer research. 2017 Jun 1;77(11):2881-92.
13. Zhang DD. The Nrf2-Keap1-ARE signaling pathway: the regulation and dual function of Nrf2 in cancer. Antioxidants & redox signaling. 2010 Dec 1;13(11):1623-6.
14. Leone A, Roca MS, Ciardiello C, Terranova-Barberio M, Vitagliano C, Ciliberto G, Mancini R, Di Gennaro E, Bruzzese F, Budillon A. Vorinostat synergizes with EGFR inhibitors in NSCLC cells by increasing ROS via up-regulation of the major mitochondrial porin VDAC1 and modulation of the c-Myc-NRF2-KEAP1 pathway. Free Radical Biology and Medicine. 2015 Dec 1;89:287-99.
15. Solis LM, Behrens C, Dong W, Suraokar M, Ozburn NC, Moran CA, Corvalan AH, Biswal S, Swisher SG, Bekele BN, Minna JD. Nrf2 and Keap1 abnormalities in non–small cell lung carcinoma and association with clinicopathologic features. Clinical cancer research. 2010 Jul 15;16(14):3743-53.
16. Bhattacharjee S, Dashwood RH. Epigenetic regulation of NRF2/KEAP1 by phytochemicals. Antioxidants. 2020 Sep 14;9(9):865.
17. Dong W, Jia Y, Liu X, Zhang H, Li T, Huang W, Chen X, Wang F, Sun W, Wu H. Sodium butyrate activates NRF2 to ameliorate diabetic nephropathy possibly via inhibition of HDAC. J Endocrinol. 2017 Jan 1;232(1):71-83.
18. Khan H, Patel S, Majumdar A. Role of NRF2 and Sirtuin activators in COVID-19. Clinical Immunology. 2021 Dec 1;233:108879.
19. Fiorentino F, Carafa V, Favale G, Altucci L, Mai A, Rotili D. The two-faced role of SIRT6 in cancer. Cancers. 2021 Mar 8;13(5):1156.
20. Krishnamoorthy V, Vilwanathan R. Silencing Sirtuin 6 induces cell cycle arrest and apoptosis in non-small cell lung cancer cell lines. Genomics. 2020 Sep 1;112(5):3703-12.
21. Tossetta G, Marzioni D. Natural and synthetic compounds in Ovarian Cancer: A focus on NRF2/KEAP1 pathway. Pharmacological Research. 2022 Jul 25:106365.
22. Liu X, Ren S, Li Z, Hao D, Zhao X, Zhang Z, Liu D. Sirt6 mediates antioxidative functions by increasing Nrf2 abundance. Experimental Cell Research. 2023 Jan 1;422(1):113409.
23. He Y, Yang G, Sun L, Gao H, Yao F, Jin Z, Zheng Z, Chen L, Wang W, Zheng N, Lin R. SIRT6 inhibits inflammatory response through regulation of NRF2 in vascular endothelial cells. International immunopharmacology. 2021 Oct 1;99:107926.
24. Ali I, Lone MN, Aboul-Enein HY. Imidazoles as potential anticancer agents. MedChemComm. 2017;8(9):1742-73.
25. Sharma P, LaRosa C, Antwi J, Govindarajan R, Werbovetz KA. Imidazoles as potential anticancer agents: An update on recent studies. Molecules. 2021 Jul 11;26(14):4213.
26. Guda R, Kumar G, Korra R, Balaji S, Dayakar G, Palabindela R, Myadaraveni P, Yellu NR, Kasula M. EGFR, HER2 target based molecular docking analysis, in vitro screening of 2, 4, 5-trisubstituted imidazole derivatives as potential anti-oxidant and cytotoxic agents. Journal of Photochemistry and Photobiology B: Biology. 2017 Nov 1;176:69-80.
27. Alghamdi SS, Suliman RS, Almutairi K, Kahtani K, Aljatli D. Imidazole as a promising medicinal scaffold: Current status and future direction. Drug Design, Development and Therapy. 2021 Jul 29:3289-312.
28. Song N, Guan X, Zhang S, Wang XK, Lu Z, Chong D, Wang JY, Yu RL, Yu W, Gu Y, Jiang T. Discovery of a Pyrrole-pyridinimidazole Derivative as Novel SIRT6 Inhibitor for Sensitizing Pancreatic Cancer Cells to Gemcitabine.
29. Dindi uma Maheswara rao, suhadha parveen sadiq, Sameer Al-Ghamdia, Naif Abdurhman Alrudiana, Salman Bin Dayelb, Abdulwahab Ali Abudermanc, Mohammad Shahidc, Thiyagarajan Ramesh, Ravikumar Vilwanathan. In-silico and In-vitro functional validation of imidazole derivatives as potential sirtuin inhibitor. Department of Biochemistry, Cancer Biology Laboratory, School of Life Sciences, Bharathidasan University, Tiruchirappalli, Tamil Nadu, India, 2023, manuscript in preparation.
30. Paglia DE, Valentine WN. Studies on the quantitative and qualitative characterization of erythrocyte glutathione peroxidase. The Journal of laboratory and clinical medicine. 1967 Jul 1;70(1):158-69.
31. Aebi H. [13] Catalase in vitro. InMethods in enzymology 1984 Jan 1 (Vol. 105, pp. 121-126). Academic press.
32. Mensor LL, Menezes FS, Leitão GG, Reis AS, Santos TC, Coube CS, Leitão SG. Screening of Brazilian plant extracts for antioxidant activity by the use of DPPH free radical method. Phytotherapy research. 2001 Mar;15(2):127-30.

33. Sharma S, Kelly TK, Jones PA. Epigenetics in cancer. Carcinogenesis. 2010 Jan 1;31(1):27-36.
34. Rashid M, Maqbool A, Shafiq N, Jardan YA, Parveen S, Bourhia M, Nafidi HA, Khan RA. The combination of multi-approach studies to explore the potential therapeutic mechanisms of imidazole derivatives as an MCF-7 inhibitor in therapeutic strategies. Frontiers in Chemistry. 2023;11.
35. Landriscina M, Maddalena F, Laudiero G, Esposito F. Adaptation to oxidative stress, chemoresistance, and cell survival. Antioxidants & redox signaling. 2009 Nov 1;11(11):2701-16.
36. Perillo B, Di Donato M, Pezone A, Di Zazzo E, Giovannelli P, Galasso G, Castoria G, Migliaccio A. ROS in cancer therapy: The bright side of the moon. Experimental & molecular medicine. 2020 Feb;52(2):192-203.
37. Glasauer A, Chandel NS. Targeting antioxidants for cancer therapy. Biochemical pharmacology. 2014 Nov 1;92(1):90-101.
38. Nimse SB, Pal D. Free radicals, natural antioxidants, and their reaction mechanisms. RSC advances. 2015;5(35):27986-8006.
39. Kharrazi H, Vaisi-Raygani A, Rahimi Z, Tavilani H, Aminian M, Pourmotabbed T. Association between enzymatic and non-enzymatic antioxidant defense mechanism with apolipoprotein E genotypes in Alzheimer disease. Clinical Biochemistry. 2008 Aug 1;41(12):932-6.
40. NavaneethaKrishnan S, Rosales JL, Lee KY. ROS-mediated cancer cell killing through dietary phytochemicals. Oxidative medicine and cellular longevity. 2019 May 14;2019.
41. Aslani BA, Ghobadi S. Studies on oxidants and antioxidants with a brief glance at their relevance to the immune system. Life sciences. 2016 Feb 1;146:163-73.
42. Chio II, Tuveson DA. ROS in cancer: the burning question. Trends in molecular medicine. 2017 May 1;23(5):411-29.
43. Zhao X, Ren X, Zhu R, Luo Z, Ren B. Zinc oxide nanoparticles induce oxidative DNA damage and ROS-triggered mitochondria-mediated apoptosis in zebrafish embryos. Aquatic Toxicology. 2016 Nov 1;180:56-70.
44. Panieri E, Saso L. Potential applications of NRF2 inhibitors in cancer therapy. Oxidative medicine and cellular longevity. 2019 Apr 11;2019.
45. Ulasov AV, Rosenkranz AA, Georgiev GP, Sobolev AS. Nrf2/Keap1/ARE signaling: Towards specific regulation. Life Sciences. 2022 Feb 15;291:120111.
46. He WJ, Lv CH, Chen Z, Shi M, Zeng CX, Hou DX, Qin S. The regulatory effect of phytochemicals on chronic diseases by targeting Nrf2-ARE signaling pathway. Antioxidants. 2023 Jan 20;12(2):236.
47. Dinkova-Kostova AT, Copple IM. Advances and challenges in therapeutic targeting of NRF2. Trends in pharmacological sciences. 2023 Jan 9.
48. Taguchi K, Yamamoto M. The KEAP1–NRF2 system in cancer. Frontiers in oncology. 2017 May 4;7:85.